Congenital Cytomegalovirus Infection of the Brain: Imaging Analysis and Embryologic Considerations

A. James Barkovich and Camilla E. Lindan

PURPOSE: To analyze the cortical gyral patterns and myelination patterns in a series of patients with congenital cytomegalovirus infections involving the central nervous system, to correlate them with known developmental events, and to develop a consistent theory regarding their embryogenesis. **METHODS:** The MR (11 patients) and CT (four patients) studies of 11 patients with congenital cytomegalovirus infections involving the brain were retrospectively reviewed. Analysis was made of myelination patterns, cortical gyral patterns, other areas of maldeveloped brain, and focal brain lesions. **RESULTS:** Lissencephaly was found in four patients. These patients had very thin cerebral cortices, extremely diminished volume of white matter, delayed myelination, small cerebella, and very enlarged lateral ventricles. Focal areas of dysplastic cortex, presumably polymicrogyria, were found in five patients. These patients had slightly thickened irregular cerebral cortices, slightly diminished volume of white matter, delayed myelination, variably small cerebella, and slightly enlarged lateral ventricles. Two patients had normal cerebral cortices, slightly diminished volume of white matter, delayed myelination, normal cerebella, and slightly enlarged lateral ventricles. Periventricular lesions, representing calcification, or perhaps blood, were seen in all groups. **CONCLUSIONS:** We postulate that the patients with lissencephaly suffer injury before 16 or 18 weeks gestational age, whereas those with regions of polymicrogyria are injured between approximately 18 and 24 weeks gestational age. Those with normal gyral patterns are probably injured during the third trimester and may have active infections at birth. Moreover, we propose that the finding of cerebellar hypoplasia and myelination delay in association with diffuse lissencephaly or cortical dysplasia should suggest the diagnosis of congenital cytomegalovirus infection.

Index terms: Cytomegalic inclusion disease; Infants, central nervous system; Infants, diseases; Brain, computed tomography; Brain, magnetic resonance

AJNR Am J Neuroradiol 15:703–715, Apr 1994

Although it has been widely reported that patients with congenital cytomegalovirus infection have associated disorders of neuronal migration and cortical organization (1–6), little has been written concerning the spectrum of cerebral cortical appearance in congenital cytomegalovirus. We had noted a wide variation of cortical gyral anomalies in those patients with congenital cytomegalovirus whom we had imaged with magnetic resonance (MR) and computed tomography (CT). We therefore undertook a detailed retrospective study of the CT and MR examinations of patients with congenital cytomegalovirus in order to document the variation in cortical gyral patterns and to attempt to explain the various gyral patterns based on associated brain abnormalities and known embryologic data.

Patients and Methods

We retrospectively reviewed MR (11 patients) and CT (four patients) of 11 patients with congenital cytomegalic inclusion disease involving the brain. Presenting signs and symptoms are listed in Table 1. Six of the infants were born prematurely (range of 33 to 36 weeks gestational age), and five were born at term. The diagnosis was established in all cases by characteristic clinical and imaging findings in conjunction with positive serologic testing for cytomegalovirus or culture of the virus from the urine

Received March 9, 1993; accepted pending revision June 21; revision received July 8.

From the University of California San Francisco, Department of Radiology, Neuroradiology Section.

Address reprint requests to A. James Barkovich, MD, Associate Professor of Radiology, University of California San Francisco, Department of Radiology, Neuroradiology Section, 505 Parnassus Ave, L-371, San Francisco, CA 94143-0628.

AJNR 15:703–715, Apr 1994 0195-6108/94/1504-0703

TABLE 1: Eleven patients with congenital cytomegalic inclusion disease involving the brain

Patient	Age	Presentation	Sequences/ Exams	Cerebral Cortex	White Matter	Ventricles	Foci of Abnormal Signal	Hemorrhage	Calcification	Posterior Fossa
1	CT, 15 days MR, 27 days	Hepatosplenomegaly Spasticity	MR: Ax 4 mm SE 3000/ 60,120 Sag 3 mm SE 616/11 Ax 4 mm SE 549/16 CT	Normal Dysplastic hippocampus	Delayed myelination, cysts anterior temporal lobes	Smoothly enlarged, left > right	Large bilateral Cb, superficial retrotrigonal, sizes from 3 x 3 mm to 15 x 15 mm. Short T1, T2, small-punctate around ventricles (supra- and infratentorial) and in basal ganglia, cerebellum Short T1, T2	Intraventricular Probable periventricular	? Periventricular	Normal
2	1 day	Microcephaly (brain weight 150 g), skin petechiae, hepatomegaly	MR: Sag 5 mm SE 617/20 Cor 5 mm SE 500/20 Ax 4 mm SE 600/20	Agyric Very thin cortex Dysplastic hippocampus	Delayed myelination Very diminished volume	Marked, smooth enlarged partially absent septum	Periventricular with short T1 size, 3–12 mm	None	Subependymal masses in cerebrum and cerebellum	Tiny cerebellum and brain stem small (10 mm) cyst
3	3 days	Microcephaly, lymphadenopathy, hepatosplenomaegaly, chorioretinitis, thromoocytopenia, anemia, petechiae	MR: Sag 4 mm SE 500/20 Ax 5 mm SE 2800/90 CT	Agyric Very thin cortex Dysplastic hippocampus	Delayed myelination Very diminished volume	Marked, smooth enlarged, absent septum, subependymal punctate short T1, T2	Punctate periventricular foci of short T1, T2	None	Subependymal foci	Tiny cerebellum
4	8 months	Seizures, developmental delay, hypotonia	MR: Sag 3 mm 616/12 Cor 5 mm 500/16 Ax 4 mm 3000/ 60,120	Bilateral cortical dysplasia. Left frontotemporoparietal and right frontotemporoparietal. Most severe posteriorly. Right parietal—subcortical short T1, dysplastic hippocampus	Delayed myelination, cysts anteromedial temporal lobes	Small cavum	None	None	Subcortical left parietal lobe	Normal

5	6 years	Developmental delay, seizures, spasticity	MR: Ax 5 mm SE 2000/40,80 CT	Bilateral frontoopercular dysplasia extending to parietal lobe	Bilateral asymetrical foci of periventricular and subcortical long T2. Diminished periventricular white matter	Smooth, slightly enlarged	Punctate, subependymal foci of short T2	None	Subependymal foci	Small cerebellum
6	8 months	Developmental delay, hypotonia, seizures	MR: Sag 5 mm SE 550/25 Ax 5 mm SE 550/25 Cor 5 mm SE 550/25 Ax 5 mm SE 3000/40,80	Bilateral frontal dysplasia extending to parietal lobe Most severe posteriorly Dysplastic hippocampus	Bilateral symmetrical foci of periventricular and subcortical long T2 in frontal and temporal lobes. Diminished white matter	Smooth, slightly enlarged	None	None	None apparent	Normal
7	2 weeks	Microcephaly, hepatomegaly, seizures	MR: Sag 6 mm SE 500/15 Ax 5 mm SE 600/15 Ax 5 mm SE 3000/60,120	Diffuse cortical dysplasia, most severe (smooth) in frontal lobes Dysplastic hippocampus	Very diminished volume Delayed myelination	Marked, smoothly enlarged	Punctate foci of short T1, T2 around frontal horns	None	Subependymal foci	Small cerebellum
8	1 day	Microcephaly, hepatosplenomegaly, petechiae, at birth. Ultrasound at 26 weeks showed large ventricles	MR: Sag 3 mm SE 500/20 Ax SE 5 mm 3000/60,120 CT	Agyric Very thin cortex Dysplastic hippocampus	Delayed myelination Very diminished volume	Marked, smoothly enlarged	Punctate, subependymal foci of short T2	None	Subependymal, subcortical, basal ganglia, cerebellar, mesencephalic	Small cerebellum Calcium dorsal midbrain
9	4 months	Seizures, microcephaly	MR: Sag 4 mm SE 600/15 Ax 4 mm SE 600/15 Ax 4 mm SE 3000/60,120	Dysplastic frontal, temporal cortex extending to parietal lobe Most severe posteriorly	Slightly diminished volume Subcortical long T1, T2	Smooth, slightly enlarged	Few subependymal punctate foci of short T2	None	Subependymal foci?	Hypogenetic vermis Slightly small hemispheres

TABLE 1: *Continued*

Patient	Age	Presentation	Sequences/ Exams	Cerebral Cortex	White Matter	Ventricles	Foci of Abnormal Signal	Hemorrhage	Calcification	Posterior Fossa
10	6 months	Microcephaly, new seizures	MR: Sag 5 mm SE 650/16 Ax 4 mm SE 600/15 Ax 4 mm SE 3000/ 60,120 Ax 5 mm SE 550/11	Dysplastic frontal, temporal cortex extending to parietal lobe Most severe posteriorly	Slightly diminished volume Subcortical long T1, T2 Delayed myelination	Smooth, slightly enlarged. Partially absent septum pellucidum	None (mild motion artifact)	None	None apparent	Small hemispheres, left > right
11	9 months	Microcephaly Developmentally normal	MR: Sag 5 mm SE 600/20 Ax 5 mm SE 3000/ 60,120 Ax 5 mm SE 550/11	Normal	Multifocal subcortical and periventricular long T1, T2	Smooth, slightly enlarged	None	None	None	Normal

Note.—Ax indicates axial; sag, saggital; cor, coronal; and SE, spin-echo.

of the child. Five children presented in the immediate neonatal period with microcephaly (four patients), hepatosplenomegaly (three patients), hepatomegaly (two patients), skin and mucous membrane petechiae (three patients), lymphadenopathy (one patient), and chorioretinitis (one patient). Six patients presented later (one at age 4 months, one at age 6 months, two at age 8 months, one at age 9 months, and one at age 19 months) with seizures (infantile spasms, five patients), developmental delay (three patients), and microcephaly (three patients).

Imaging studies were performed during the first 2 weeks of life in four of the five patients diagnosed in the neonatal period and at ages 15 days (CT) and 27 days (MR) in the fifth. Of the six patients diagnosed later in infancy, five were imaged at the time of presentation and the sixth (patient 5) at 6 years of age. CT scans were obtained in four patients (Table 1) and consisted of contiguous 10-mm axial sections through the brain without the use of intravenous contrast. The MR studies were performed at 1.5 T and included sagittal 3- to 6-mm (1-mm gap) spin-echo 500–650/11–25/1–2 (repetition time/echo time/excitations) in 10 patients, axial 4- to 5-mm (1-mm gap) spin-echo 549–600/15–25 in seven patients, axial 4- to 5-mm (2- to 2.5-mm gap) spin-echo 2000–3000/30–60,80–120 images in nine patients, and coronal 5-mm (1-mm gap) spin-echo 500–550/16–25 images in three patients. The acquisition matrix was 128 to 192 × 256. Intravenous contrast was not used in any of the patients.

Imaging studies were assessed for cerebral cortical pattern and thickness, white matter volume (assessed subjectively), state of myelination (as compared with normal standards) (7), ventricular size and shape, cerebellar size and development, and the presence of parenchymal masses, hemorrhage, or calcification. Differentiation of hemorrhage from calcification was problematic, as will be addressed in the Discussion.

Patient 2 died at 3 days of age from complications of the cytomegalic inclusion disease and underwent a limited autopsy.

Results

The cerebral cortical gyral pattern was abnormal in nine patients. In three, the cortex was abnormally thin and essentially agyric (Fig 1), showing no sulci other than primitive, vertically oriented Sylvian fissures. In the other six, the cortex showed multiple confluent areas of thickening with irregular cortical surface and irregularity of the gray matter–white matter junction (Figs 2-4). The frontal cortex, extending posteriorly to include the perirolandic regions, was dysplastic in all six patients with localized dysplasia. The temporal lobe was involved in four of these patients (Fig 3A). In addition, the parietal region of patient 4 had a curvilinear focus of T1 shortening (Fig 3C) at the gray matter–white matter junction,

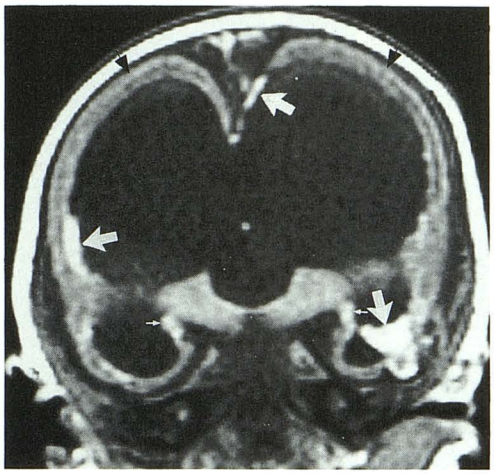

A

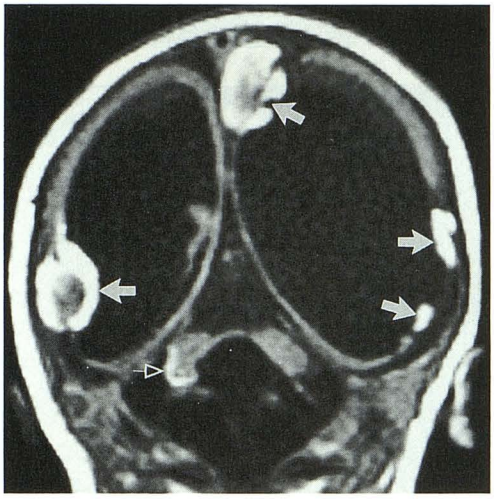

B

Fig. 1. Patient 2.

A, Coronal spin-echo 500/20 image shows an agyric brain with a very thin cortex (*black arrows*). Foci of short T1 (*large white arrows*), proved to be calcium at autopsy, are present in multiple subependymal sites. The hippocampi (*small white arrows*) are shrunken and calcified.

B, The cerebellum is markedly small and demonstrates some surface calcification (*open white arrow*). Large masses of calcium (*closed white arrows*) line the lateral ventricles.

believed to represent calcification or laminar necrosis (8, 9).

The hippocampal formations were abnormal in all seven patients in whom they could be adequately visualized. In all of these, the temporal horns of the lateral ventricles were significantly enlarged, and the hippocampi themselves were vertical (as compared with their normal horizontal orientations) and abnormally small (Fig 1A). The hippocampal region demonstrated a short T1 in patient 2 (Fig 1A), verified as calcification at autopsy.

Myelination was delayed or absent in 10 patients. In the newborn patients, this was manifest on the MR studies as absence of T1 and T2 shortening in the posterior brain stem and the posterior limbs of the internal capsules, regions in which myelination is present in healthy newborns. In patients 6, 9, 10, and 11 the hypomyelination was rather subtle, manifest as lack of T1 and T2 shortening in the middle and peripheral portions of the centra semiovale (Fig 4). The deep white matter structures, the corpus callosum, and the internal capsules appeared normally myelinated. The white matter in patient 5 was completely myelinated but showed regions of T2 prolongation (Fig 2A), presumably resulting from tissue destruction, in the subcortical white matter. On the accompanying CT scan, these regions were hypodense (Fig 2B). Volume of white matter was judged to be diminished in the cerebral hemispheres in this patient and nine others (Figs 1, 2, and 5), implying that either lack of formation or destruction of white matter had occurred in these patients. Ventricular enlargement was present in all 10 patients who had diminished cerebral hemispheric white matter. In all of these patients, the ventricular walls were smoothly expanded, without focal irregularities.

There were areas with T1 and T2 characteristics identical to cerebrospinal fluid, presumably cysts, in the anterior temporal lobes, anterior to the temporal horns of the lateral ventricles, in four patients (Figs 5F and 5G). These were separated from the ventricle by only a thin membrane. A small amount of white matter separated the cyst from the cerebral cortex in two patients; however, in the other two, the cysts extended all the way to the temporal cortex.

Well-defined signal abnormalities of variable size, ranging from 1 to 15 mm in diameter (Figs 1 and 5) were seen in the cerebral hemispheres of seven patients. In an eighth patient (patient 10), no abnormal foci were seen; however, some motion artifact was present, possibly obscuring small abnormalities. Most foci were cerebral, periventricular, or subependymal in location, but there were subcortical, cerebellar, and basal ganglia foci in one patient (patient 1, Fig 5), subcortical, basal ganglia, cerebellar, and mesencephalic foci in another, and subependymal and cerebellar foci in a third. In five patients, the masses exhibited short T1 and T2 relaxation times with respect to brain tissue. CT, obtained in three of these patients, showed high attenuation, compatible with either calcium or blood. A fourth patient

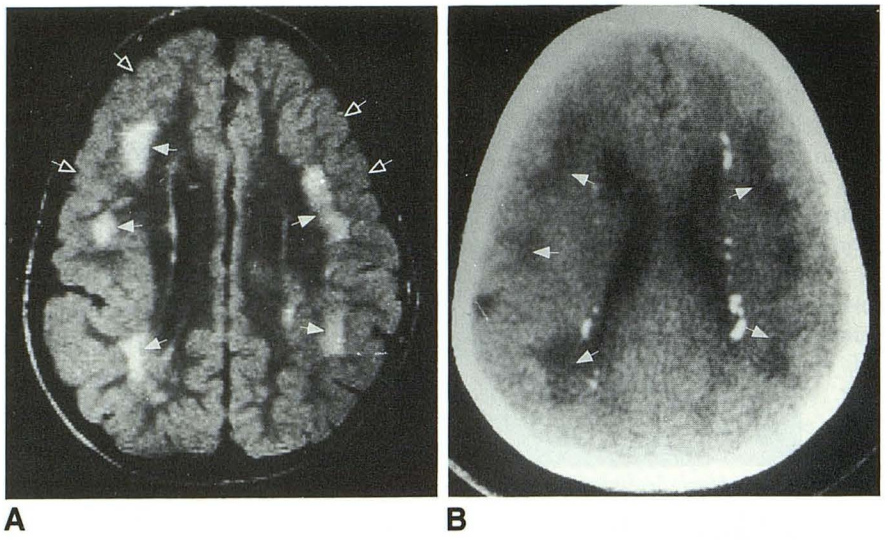

Fig. 2. Patient 5.

A, Axial spin-echo 2000/40 image shows dysplastic cortex involving most of both frontal lobes (*open arrows*) and asymmetric foci of long T2 (*closed arrows*) in the subcortical regions bilaterally.

B, Axial noncontrast CT through the same level as A shows subependymal calcification and regions of hypoattenuation (*arrows*) that correspond to the areas of long T2.

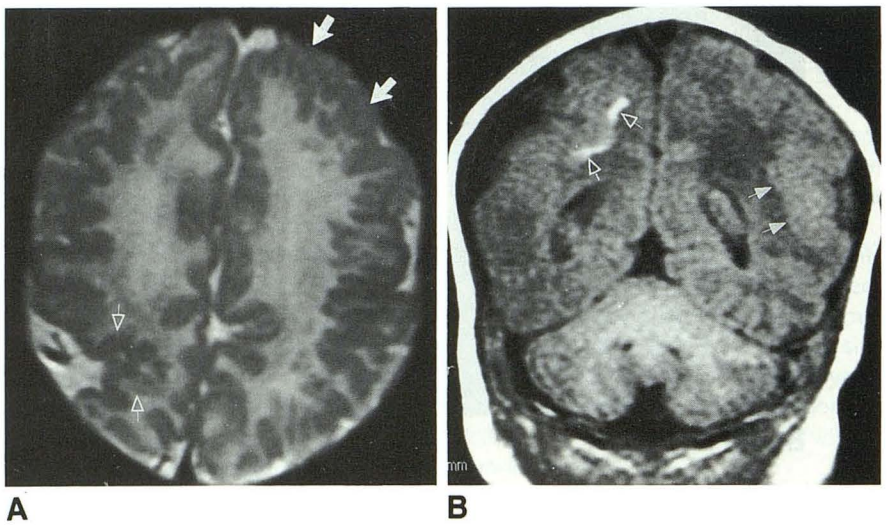

Fig. 3. Patient 4.

A, Axial spin-echo 3000/120 image shows an abnormal gyral pattern in both frontal lobes, most marked in the anterior left frontal region (*closed arrows*). An infolding of abnormal cortex is present in the right parietal region (*open arrows*).

B, Coronal spin-echo 600/15 image shows focal T1 shortening (*open arrows*) at the gray matter–white matter junction in the right parietal lobe, presumably calcification. The left temporoparietal cortex is abnormally thickened (*closed arrows*).

(patient 2), studied only by MR (Fig 1), was found to have calcium, but no blood, in the location of these masses at autopsy. It is of interest that, in patient 1, the MR showed punctate, periventricular foci better than the CT (Figs 5B–5D). Presumably, these foci represented subacute hemorrhage and not calcification, as CT is known to be much more sensitive in the detection of calcium than MR. Supporting this assumption is the fact that patient 1 had intraventricular blood and, presumably, had an active infection at birth.

Hemorrhage was identified definitely in only one patient and was intraventricular (Fig 5). However, we cannot be certain that some of the foci of T1 and T2 shortening that we are ascribing to calcium are not, in fact, partially or wholly hemorrhagic. In fact, as alluded to above, we suspect the parenchymal foci of short T1 in patient 1 are hemorrhages.

The cerebellum was judged to be small in seven patients. In two patients, the diminished cerebellar size was dramatic (Fig 1) and the cerebellum appeared incompletely formed, whereas in the other five patients, the diminution in size was less dramatic, and although small, the cerebellum appeared completely formed. None of the affected cerebella had any focal abnormalities or any features of infarction.

Discussion

Congenital cytomegalovirus disease is the most common serious viral infection among newborns in the United States (10). Congenital cytomeg-

A B

Fig. 4. Patient 9. The pattern seen in this patient was the most common in this series.

A, Axial spin-echo 600/15 image shows ventricular enlargement, abnormal hypointensity of the subcortical white matter, and an abnormal gyral pattern in the frontal lobes bilaterally. The gyral pattern is somewhat difficult to assess, because the cortex and underlying white matter are nearly isointense.

B, Axial spin-echo 3000/120 image more clearly shows the bilateral frontal cortical gyral abnormalities, with shallow sulci, thickened cortex, and irregular gray matter–white matter junction.

alovirus infection occurs in approximately 40 000 newborns each year, or approximately 1% of all births. Of these, 10% have the various hematologic, neurologic, and developmental symptoms and signs that define the disease, including hepatosplenomegaly, microcephaly, impaired hearing, and small head size. An additional 10% to 15% of infected infants subsequently develop neurologic or developmental abnormalities in the first year of life (11). In a large recent study from the congenital cytomegalovirus disease registry (12), hepatosplenomegaly (52%) and petechiae (51%) were found to be the most common clinical signs among affected children. Severe permanent neurologic conditions were found in 55%, including intracranial calcifications (43%), microcephaly (27%), chorioretinitis (15%), and seizures (10%). "Less severe neurological abnormalities" (not specified) were found in 31%, and hearing loss of varying degree was noted in 27%.

Although the sonographic findings of congenital cytomegalovirus (2, 13, 14) and the CT findings (2, 15, 16) are better defined, MR findings have recently been reported (2, 3, 6, 17, 18). MR findings in congenital cytomegalovirus have included cerebellar hypoplasia (2, 18, 19), cerebral atrophy (2), cortical gyral anomalies (3, 6, 18), dilated ventricles (6, 17), large subarachnoid spaces (6), T1 and T2 prolongation of the white matter and delayed myelination (6, 17, 18), pachygyria (17), paraventricular cysts (6), and intracranial calcification (10%) (6, 17). We observed similar anomalies; in addition, however, our scans of our patients demonstrated hemorrhage, focal white matter injury, and hippocampal abnormalities. Moreover, gyral anomalies varied from complete lissencephaly to localized cortical dysplasia.

There was abnormal T1 and T2 prolongation of the white matter in eight of the 10 patients. In patients 2, 3, 7, and 8, who had lissencephaly with thin cerebral cortices and marked diminution of cerebral white matter (Fig 1), this appearance may be the result of diffuse postencephalitic gliosis, as suggested by Titelbaum et al (3). However, patients 1, 4, 9, 10, and 11 had little diminution in the amount of white matter and had areas of normal-appearing cortex (Figs 3 and 4) beneath which the white matter had diffusely prolonged T1 and T2 relaxation times. The mildly diminished volume of white matter and the normal-appearing overlying cortex would suggest that the encephalitic process was not locally very severe; therefore, we concur with Boesch et al (6) that the T1 and T2 prolongation most likely results, at least in part, from delayed or deficient myelination.

Delayed myelination is expected in patients with congenital cytomegalovirus on a theoretical basis, as much of the brain damage from the infection is in the periventricular region, the region of the germinal matrix. The lineage of the cells being formed in the germinal zones differs depending upon the gestational age of the fetus (20–23). Neurons are formed from about 8 weeks gestational age until 16 to 20 weeks (exact timing is not clearly established); their migration to the cerebral cortex continues until about 24 to 26 weeks and is followed by a period of cortical

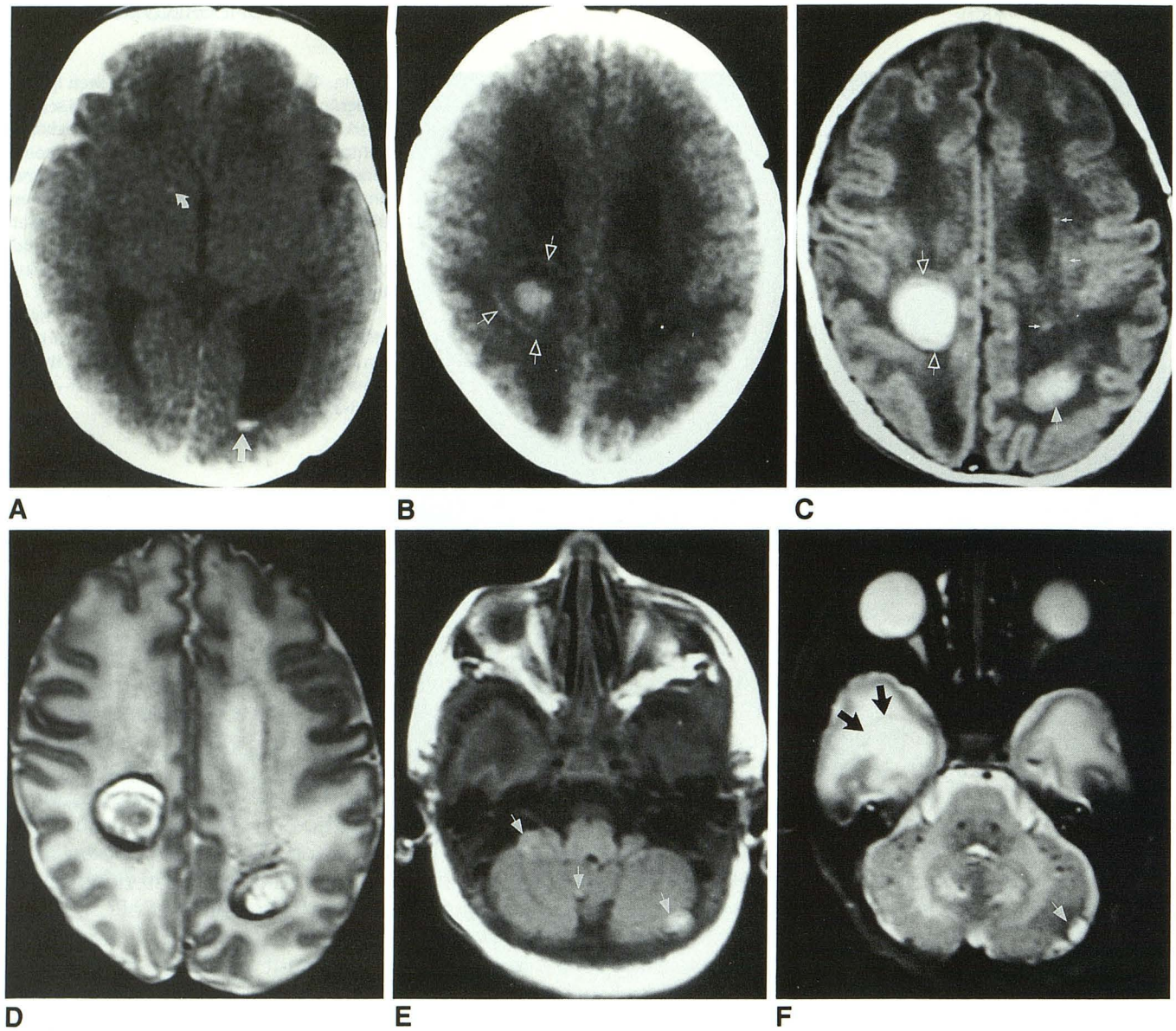

Fig. 5. Patient 1.

A, Axial CT shows blood layering in the occipital horn of the left lateral ventricle (*large arrow*). A small focus of hemorrhage is present in the right basal ganglia region (*small arrow*).

B, Axial CT at the level of the top of the lateral ventricles. A circular region of hemorrhage is present in the right hemisphere with a rim of high attenuation (*arrows*) surrounding it.

C, Axial spin-echo 549/16 image at the same level as B shows marked T1 shortening from hemorrhage in the right hemisphere (*open arrows*) corresponding to the high attenuation CT focus. A second area of hemorrhage (*closed arrow*) that was not seen on the CT is present in the left parietal lobe. A few smaller foci are present (*small arrows*).

D, Axial spin-echo 3000/120 image at the same level as B and C shows that both of the larger lesions identified in C have a rim of marked T2 shortening surrounding heterogeneous signal in the center. Multiple punctate foci of hemorrhage, manifest as regions of T2 shortening, that were not identified on the CT or T1-weighted MR are present along the margins of the ventricle and in the frontal white matter.

E, Axial spin-echo 549/16 image at the level of the medulla shows three areas of hemorrhage (*arrows*) in the cerebellum.

F, Axial spin-echo 3000/120 image 6 mm rostral to E shows multiple punctate foci of hemorrhage that were not apparent on the CT scan or on the short-repetition-time/short-echo-time MR images. The focus of hemorrhage in the lateral left cerebellar hemisphere in E has a high signal intensity (*white arrow*) on this image. A cyst in the right anterior temporal lobe (*black arrows*) is faintly seen.

G, Sagittal spin-echo 616/11 image shows the right temporal lobe cyst (*arrow*) surrounded by low intensity white matter, anterior and inferior to the temporal horn of the lateral ventricle.

organization (22). Near the end of the period of neuronal production, astrocyte generation begins (20, 21, 24). The germinal zone attains its maximum size at 26 weeks (20, 25), at which time astrocytes are the predominant cell type being formed (20). The early stages of astrocyte formation and migration seem to be necessary for normal cortical organization (21). Oligodendrocytes are produced by differentiation of astrocytes produced in the first half of the third trimester (25) (van der Knaap M, Myelination and Myelin Disorders: a Magnetic Resonance Study in Infants, Children, and Young Adults, Thesis, Free University of Amsterdam and University of Utrecht, 1991), before the germinal zone becomes depleted at 32 to 34 weeks. As a result of this timing of cell production, an early injury to the germinal zone is likely to produce a reduction in both neurons and glia, whereas an injury after 22 to 24 weeks is expected to result in the production of a normal number of neurons but a reduced number of glia. Moreover, an injury after 24 to 26 weeks would not be expected to affect the migration of neurons to the cerebral cortex (they have completed the migration). Injury late in the migration phase or in the organizational phase, if vascular in nature, is believed to result in polymicrogyria (22, 25). Therefore, in order to discuss the interrelationship of the white matter and cortical anomalies in patients with congenital cytomegalovirus, a discussion of the most likely cause of brain injury in congenital cytomegalovirus is necessary.

Some debate exists in the literature as to the mechanism of brain injury in congenital cytomegalovirus. The earliest and most widely repeated theories stated that cytomegalovirus has a special affinity for the immature cells within the germinal zone and that the loss of periventricular brain tissue and the abnormalities of the cerebral cortex were the result of the injury to the germinal zone and the cells produced therein (4, 15, 26, 27). Marques-Dias et al (28), however, noted that no neuropathologic differences were apparent histologically between the cortical anomalies of patients with cytomegalovirus and those with polymicrogyria of other causes. Furthermore, they noted no correlation between the location of the periventricular injuries and the location of the cortical anomalies. Finally, they noted no difference between the periventricular white matter injuries of patients with cytomegalovirus and those of patients with congenital toxoplasmosis infection or with ischemic periventricular white matter calcifications, as described by Banker and Larroche (29). Moreover, animal models indicate that polymicrogyria is the result of a localized cortical injury that disrupts cortical organization (30–33). The injury may involve the developing cortex itself (30, 31, 33) or may be limited to the more superficial pial-glial membrane, which aids in cortical organization (32, 34). Polymicrogyria has not been shown to result from germinal matrix injury.

In contradistinction to direct brain injury by the virus, Marques-Dias et al postulated that the brain injury in patients with congenital cytomegalovirus was the result of ischemia (28). In support of their postulate, they noted that thrombotic vasculitis caused by cytomegalovirus has been seen in the placenta (35, 36) and in the fetal lung (35). Moreover, they pointed out that cytomegalovirus inclusions seem to be preferentially present in proliferating capillary endothelia in animal models (37). More recent literature supports the causative role of cytomegalovirus in vascular injury (38), thrombosis (39), and retinal angiitis (40). However, although they found numerous cytomegalovirus inclusions in capillaries, Marques-Dias et al (28) found no evidence of thrombosis or alteration of vessel walls and did not note any randomly multifocal lesions, as would be expected from a vasculitic process. They found the distribution of lesions more consistent with systemic insufficiency of fetal circulation. Therefore, they postulated that the injuries were the result of a placentitis and secondary chronic perfusion insufficiency.

The patterns of brain injury in some of the patients in our series are compatible with systemic vascular insufficiency as the underlying cause of brain damage. The dysplastic cortex tended to be symmetric and to involve the opercular region, a pattern we and others (41–43) have noted in polymicorgyria secondary to fetal hypotension. Using the known timing of cell formation in the germinal zones (discussed earlier), we estimate that patients 2, 3, and 8, who had completely smooth (agyric) brains, extremely thin cerebral cortices, and markedly diminished cerebral hemispheric white matter, presumably were infected while neurons were being formed and in the early stages of migrating to the cerebral cortex (probably before 16 or 18 weeks gestation). Injury at this time would result in few neurons arriving at the cortex to establish axonal ramifications with the remainder of the brain; moreover, the destroyed germinal zone would be

unable to produce a sufficient number of oligodendrocytes to myelinate the axons that had formed. We estimate that patients 4, 5, 6, 7, 9, and 10, who had symmetrical frontotemporoparietal cortical dysplasia (presumably polymicrogyria) and delayed myelination with relatively little ventricular dilatation, were infected later, at a time when neuronal migration was nearly completed and neuronal organization was taking place (probably about 18 to 24 weeks) (22, 24, 44). The fact that this pattern of injury is nearly identical to the most common pattern of cortical dysplasia/polymicrogyria in patients without a history of cytomegalovirus (42, 45, 46) also supports a vascular cause of the brain damage in cytomegalovirus disease, because polymicrogyria is presumed to be caused primarily by ischemia (22, 25, 47). Patients 1 and 11, who had normal gyral patterns, presumably were infected during the third trimester, after cortical organization is completed. Patient 1, who had intraventricular and, presumably, periventricular hemorrhage detected on his scans, may have had ongoing infection (cytomegalovirus cerebritis) at birth, as reported by Bray et al (48) and Bale et al (49). Because the cerebritis presumably lasts several weeks, or even months (2, 48), and myelination continues for years after birth (50, 51), the presence of both delayed myelination and active infection in a term infant is predictable.

The MR appearance of delayed myelination and a thin cortex in a patient with agyria (such as patients 2, 3, and 8) should strongly suggest the possibility of cytomegalovirus infection, because the most common form of agyria, type 1 lissencephaly, is usually associated with a thick layer of neurons lying central to a "cell-sparse" zone (52, 53). Moreover, the white matter in type 1 lissencephaly is almost always normally myelinated (53). Finally, the cerebellum is typically normal in type 1 lissencephaly but was abnormally small in all three of the patients with smooth brains in this series. Differentiation from microcephalia vera, a condition caused by premature exhaustion of the germinal matrix (22, 25, 54), may be difficult on the basis of imaging studies; however, the associated hepatosplenomegaly and skin petechiae of cytomegalovirus and the family history (microcephalia vera is thought to have an autosomal recessive pattern of inheritance) should allow differentiation.

Differentiation of type 2 lissencephaly, as is seen in Walker-Warburg syndrome and in Fukuyama congenital muscular dystrophy, from the patterns of cortical dysplasia seen in patients 6, 7, 9, and 10, is somewhat more difficult using imaging criteria alone. Both disorders have myelination delay, cerebellar anomalies, and thickening of the cerebral cortex with irregular gyral patterns (22, 55–58). Absence of the characteristic bundles of dysplastic neurons plunging into the white matter at the gray matter–white matter junction, a typical finding in type 2 lissencephaly (22), should help to differentiate the disorders. In addition, patients with Walker-Warburg syndrome have callosal hypogenesis or agenesis, persistent primary hypertrophic vitreous, hydrocephalus, and, commonly, occipital cephaloceles that should allow differentiation. Moreover, neither Walker-Warburg syndrome nor Fukuyama congenital muscular dystrophy are reported to have subependymal or periventricular calcifications, as were seen in two of our patients. Finally, hepatosplenmegaly and skin petechiae, common in cytomegalovirus disease, are not reported with type 2 lissencephaly.

The pattern of brain injury correlated with age of patient presentation in that the patients with agyria all presented at birth and died by the age of 4 months, whereas those with a more pachygyric or polymicrgyric pattern presented later in infancy with seizures and developmental delay, presumably caused by the cortical and myelination anomalies. The timing of presentation is in agreement with our theory regarding timing of infection in that those patients infected earlier, when organogenesis was still in progress, would presumably have more severe multiorgan involvement and have more difficulty adapting to the extrauterine environment. The exception to the trend of earlier presentation of more severe brain injury was patient 1, who presented at birth despite a normal gyral pattern. However, as has been discussed, patient 1 is presumed to have had an active infection at birth and, therefore, would be expected to be sicker than those whose infections were no longer active.

The observation that the cerebellum was abnormally small in eight of the 11 patients in this series may be of some diagnostic significance. Although Dobyns (56, 59) has reported a few patients with lissencephaly and cerebellar hypoplasia, most disorders of neuronal migration and organization and most destructive brain disorders have normal-appearing cerebelli on imaging studies. In hypoxic-ischemic injury, for example, sparing of the cerebellum is a classic imaging finding that is used to establish the diagnosis (60–64).

We suggest that the presence of cerebellar hypoplasia on MR studies, when seen in association with cortical dysplasia or lissencephaly, myelination delay, and diminished white matter, should prompt strong consideration of a diagnosis of congenital cytomegalovirus infection.

Seven patients had temporal lobe abnormalities, including hippocampal dysplasia and anterior temporal lobe cysts. The hippocampal dysplasia, manifest as vertical (as opposed to the normal horizontal) orientation of the hippocampus (Fig 1A), is similar to the pattern described by Baker and Barkovich (65) in developmental anomalies such as type I lissencephaly and agenesis of the corpus callosum. Therefore, it is likely that this hippocampal appearance is a result of an arrest of hippocampal development by the infection. It is a nonspecific finding. The significance of the temporal lobe cysts (Figs 5F and 5G) is uncertain; they were seen only in four patients. They are probably the result of localized tissue destruction. Analysis of more cases is necessary to determine whether this finding is at all specific for cytomegalovirus.

Periventricular foci of signal abnormality were seen in eight of the 11 patients in this study (Figs 1 and 5). The lesions were globular in patients 1 and 2, ranging in size from 3 to 15 mm in diameter. The lesions in patient 1 had short T1 and T2 relaxation times; patient 2 was imaged only with short-repetition-time/short-echo-time spin-echo images, so only short T1 relaxation time was established. Based on the MR appearance of these lesions, we suspected that they were foci of hemorrhage; however, autopsy of patient 2 revealed only periventricular calcification, with no evidence of blood. The difficulty in distinguishing hemorrhage from calcium on MR has been discussed both theoretically (9) and in reference to injuries of the pediatric brain (62). Cytomegalovirus infection seems to be another category in which the differentiation of subacute blood from calcium is problematic. The difficulty was compounded in patient 1, in whom hemorrhage was clearly present within the lateral ventricles (Fig 5A), and who, as suggested earlier, probably had an active infection at birth. Although the MR characteristics of the lesions in this patient were identical to those in patient 1, the CT characteristics suggest that they were hemorrhagic. Parenchymal injury can clearly progress postnatally in patients with congenital cytomegalovirus (2, 48, 49); thus, the possibility cannot be excluded that some of the lesions were initially hemorrhagic and evolved into calcified lesions via dystrophic calcification. Whether this transformation would be detectable by MR is unknown.

Punctate periventricular lesions were present on MR images of five patients. In two, the lesions had short T1 and short T2 relaxation times compared with surrounding white matter, whereas in three patients, the lesions could not be distinguished from surrounding brain on T1-weighted images, but had short T2 compared with surrounding brain. We suspect that most of these punctate foci represent calcification, although some may represent residual blood or blood breakdown products similar to the periventricular foci in patient 1 (Fig 5). Calcified subependymal foci were clearly shown on the CT of patient 5 but were not seen on the accompanying MR (Fig 2). Although the MR of patient 5 was relatively old, this observation once again proves the advantage of CT over MR in the detection of small, punctate calcification. The presence of calcification, however, does not seem essential to make the diagnosis.

In summary, we have described a wide spectrum of cortical anomalies, ranging from complete agyria to diffuse polymicrogyria to grossly normal, in infants and children with congenital cytomegalovirus infections. We have proposed an explanation, based on the timing of the infection during gestation, to explain this spectrum. Moreover, we have described parenchymal lesions, of variable size, that may represent calcifications or hemorrhage and may be difficult to distinguish by MR imaging alone. Finally, we have noted myelination delay and cerebellar hypoplasia as consistent abnormalities in congenital cytomegalovirus and suggested that these findings may be valuable in differentiating congenital infection from various genetic and sporadic congenital disorders.

Acknowledgments

We thank Erik Gaensler, MD, for the use of cases 9 and 10, and Wallace Peck, MD, for the use of case 2.

References

1. Bignami A, Appicciutoli L. Micropolygyria and cerebral calcification in cytomegalic inclusion disease. *Acta Neuropathol* 1964;4:127–137
2. Perlman JM, Argyle C. Lethal cytomegalovirus infection in preterm infants: clinical, radiological, and neuropathological findings. *Ann Neurol* 1992;31:64–68

3. Titelbaum DS, Hayward JC, Zimmerman RA. Pachygyriclike changes: topographic appearance at MR imaging and CT and correlation with neurologic status. *Radiology* 1989;173:663–667
4. Friede R, Mikolasek J. Postencephalitic porencephaly, hydranencephaly or polymicrogyria. A review. *Acta Neuropathol* 1978;43:161–168
5. Crome L, France N. Microgyria and cytomegalic inclusion disease in infancy. *J Clin Pathol* 1959;12:427–434
6. Boesch C, Issakainen J, Kewitz G, Kikinis R, Martin E, Boltshauser E. Magnetic resonance imaging of the brain in congenital cytomegalovirus infection. *Pediatr Radiol* 1989;19:91–93
7. Barkovich AJ, Kjos B, Jackson Jr D, Norman D. Normal maturation of the neonatal and infant brain: MR imaging at 1.5 T. *Radiology* 1988;166:173–180
8. Boyko O, Burger P, Shelburne J, Ingram P. Non-heme mechanisms for T1 shortening: pathologic, CT, and MR elucidation. *AJNR Am J Neuroradiol* 1992;13:1439–1445
9. Henkelman M, Watts J, Kucharczyk W. High signal intensity in MR images of calcified brain tissue. *Radiology* 1991;179:199–206
10. Alford C, Stagno S, Pass R, Britt W. Congenital and perinatal cytomegalovirus infections. *Rev Infect Des* 1990;12 (suppl 7):S745–S753
11. Yow M. Congeintal cytomegalovirus disease: a now problem. *J Infect Dis* 1989;159:163–167
12. Dobbins JG, Stewart JA, Demmler GJ. Surveillance of congenital cytomegalovirus disease, 1990–1991. Collaborating Registry Group. *MMWR CDC Surveill Summ* 1992;41:35–39
13. Butt W, Mackey R, DeCrespigny L, et al. Intracranial lesions of congenital cytomegalovirus infection detected by ultrasound scanning. *Pediatrics* 1984;73:611–615
14. Dykes F, Ahmann P, Lazzara A. Cranial ultrasound in the detection of intracranial calcifications. *J Pediatr* 1982;100:406–408
15. Barkovich AJ. Infections of the nervous system. In: Barkovich AJ, ed. *Pediatric neuroimaging.* New York: Raven, 1990:293–325
16. Bale J, Bray P, Bell W. Neuroradiographic abnormalities in congenital cytomegalovirus infection. *Pediatr Neurol* 1985;1:42–45
17. Hayward JC, Titelbaum DS, Clancy RR, Zimmerman RA. Lissencephaly-pachygyria associated with congenital cytomegalovirus infection. *J Child Neurol* 1991;6:109–114
18. Sugita K, Ando M, Makino M, Takanashi J, Fujimoto N, Niimi H. Magnetic resonance imaging of the brain in congenital rubella virus and cytomegalovirus infections. *Neuroradiology* 1991;33:239–242
19. Volpe J. Viral and related intracranial infections. In: Volpe J, ed. *Neurology of the newborn.* Philadelphia: Saunders, 1987:548–595
20. Jammes J, Gilles F. Telencephalic development: matrix volume and isocortex and allocortex surface areas. In: Gilles F, Leviton A, Dooling E, eds. *The developing human brain.* Boston: Wright, 1983:87–93
21. Gressens P, Richelme C, Kadhim H, Gadisseux J-F, Evrard P. The germinative zone produces the most cortical astrocytes after neuronal migration in the developing mammalian brain. *Biol Neonate* 1992;61:4–24
22. Barkovich AJ, Gressens P, Evrard P. Formation, maturation, and disorders of brain neocortex. *AJNR Am J Neuroradiol* 1992;13:423–446
23. Altman J, Bayer S. Horizontal compartmentation in the germinal matrices and intermediate zone of the embryonic rat cerebral cortex. *Exp Neurol* 1990;107:36–47
24. Sidman RL, Rakic P. Development of the human central nervous system. In: Haymaker W, Adams RD, eds. *Histology and histopathology of the nervous system.* Springfield: Thomas, 1982:3–145
25. Evrard P, de Saint-Georges P, Kadhim H, Gadisseux J-F. Pathology of prenatal encephalopathies. In: French J, ed. *Child neurology and developmental disabilities.* Baltimore: Brookes, 1989:153–176
26. Naeye R. Cytomegalic inclusion disease: the fetal disorder. *Am J Clin Pathol* 1967;47:738–744
27. Mercer R, Luse S, Guyton D. Clinical diagnosis of generalized cytomegalic inclusion disease. *Pediatrics* 1953;11:502–514
28. Marques-Dias M, Harmant-van Rijckevorsel G, Landrieu C, et al. Prenatal cytomegalovirus disease and cerebral microgyria: evidence for perfusion failure, not disturbance of histogenesis, as the major cause of fetal cytomegalovirus encephalopathy. *Neuropediatrics* 1984;15:18–24
29. Banker B, Larroche J. Periventricular leukomalacia of infancy. *Arch Neurol* 1962;7:386–410
30. Dvorak K, Feit J. Migration of neuroblasts through partial necrosis of the cerebral cortex in newborn rats. Contribution to the problems of morphological development and developmental period of cerebral microgyria. *Acta Neuropathol* 1977;38:203–212
31. Dvorak K, Feit J, Jurankova Z. Experimentally induced focal microgyria and status verrucosis deformis in rats—pathogenesis and interrelation, histological and autoradiographical study. *Acta Neuropathol* 1978;44:121–129
32. Humphreys P, Rosen G, Press D, Sherman G, Galaburda A. Freezing lesions of the developing rat brain: a model for cerebral microgyria. *J Neuropathol Exp Neurol* 1991;50:145–160
33. Suzuki M, Choi B. Repair and reconstruction of the cortical plate following closed cryogenic injury to the neonatal rat cerebrum. *Acta Neuropathol* 1991;82:93–101
34. Rosen G, Sherman G, Richman J, Stone L, Galaburda A. Induction of molecular ectopias by puncture wounds in newborn rats and mice. *Dev Brain Res* 1992;67:285–291
35. Benirschke K, Mendoza G, Bazeley P. Placental and fetal manifestations of CMV. *Virchows Arch [B]* 1974;16:121–139
36. Altschuler G, McAdams J. CMV inclusion disease of a 19 week fetus. *Am J Obstet Gynecol* 1971;111:295–298
37. Vogel F. Enhanced susceptibility of proliferating endothelium to salivary gland virus under naturally occurring and experimental conditions. *Am J Pathol* 1958;34:1069–1079
38. Span AH, Grauls G, Bosman F, van BC, Bruggeman CA. Cytomegalovirus infection induces vascular injury in the rat. *Atherosclerosis* 1992;93:41–52
39. Jenkins RE, Peters BS, Pinching AJ. Thromboembolic disease in AIDS is associated with cytomegalovirus disease (letter). *AIDS* 1991;5:1540–1542
40. Spaide R, Vitale A, Toth I, Oliver J. Frosted branch angiitis associated with cytomegalovirus retinitis. *Am J Ophthalmol* 1992;113:522–528
41. Bankl J, Jellinger K. Zentralnervose Schaden nach fetaler Kohlenoxidvergiftung. *Beitr Pathol Anat* 1967;135:350–376
42. Barth PG. Disorders of neuronal migration. *Can J Neurol Sci* 1987;14:1–16
43. Hallervorden J. Ueber eine kohlenoxydvergiftung im fetalleben mit entwicklunsstorung der hirnrinde. *Allg Z Psychiatr* 1949;124:289–298
44. Barkovich AJ, Lyon G, Evrard P. Formation, maturation, and disorders of white matter. *AJNR Am J Neuroradiol* 1992;13:447–461
45. Barkovich AJ, Kjos B. Schizencephaly: correlation of clinical findings with MR characteristics. *AJNR Am J Neuroradiol* 1992;13:85–94
46. Barkovich AJ, Kjos B. Nonlissencephalic cortical dysplasia: correlation of imaging findings with clinical deficits. *AJNR Am J Neuroradiol* 1992;13:95–103
47. Richman DP, Stewart RM, Caviness BS. Cerebral microgyria in a 27 week fetus: an architectonic and topographic analysis. *J Neuropathol Exp Neurol* 1974;33:374–384
48. Bray P, Bale J, Anderson R, Kern E. Progressive neurological disease associated with chronic cytomegalovirus infection. *Ann Neurol* 1981;9:499–502
49. Bale J, Sato Y, Eisert D. Progressive postnatal subependymal necrosis in infant with congenital cytomegalovirus infection. *Pediatr Neurol* 1986;2:367–370

50. Yakovlev P, Lecours A. The myelogenetic cycles of regional maturation of the brain. In: Minkowski A, ed. *Regional development of the brain in early life*. Oxford: Blackwell, 1967:3–70
51. Brody B, Kinney H, Kloman A, Gilles F. Sequence of central nervous system myelination in human infancy. I. An autopsy study of myelination. *J Neuropathol Exp Neurol* 1987;46:283–301
52. Aicardi J. The agyria-pachygyria complex: a spectrum of cortical malformations. *Brain Dev* 1991;13:1–8
53. Barkovich AJ, Koch T, Carrol C. The spectrum of lissencephaly: report of ten cases analyzed by magnetic resonance imaging. *Ann Neurol* 1991;30:139–146
54. Parain D, Gadisseux J, Henocq A, Tayot J, Evrard P. Diagnostic prenatal et etude d'une microcephalia vera a 26 semaines de gestation. In: Szliwowski H, Bormans J, eds. *Progres en neurologie pediatrique*. Brussels: Prodim, 1985:235–236
55. Bordarier C, Aicardi J, Boutieres F. Congenital hydrocephalus and eye abnormalities with severe developmental brain defects: Warburg's syndrome. *Ann Neurol* 1984;16:60–65
56. Dobyns WB, Kirkpatrick JB, Hittner HM, Roberts RM, Kretzer FL. Syndromes with lissencephaly: 2. Walker-Warburg and cerebral ocular muscular syndromes and a new syndrome with Type 2 lissencephaly. *Am J Med Genet* 1985;22:157–195
57. Takada K, Nakamura H, Takashima S. Cortical dysplasia in Fukuyama congenital muscular dystrophy: a Golgi and angio architect tonic analysis. *Acta Neuropathol* 1988;76:170–178
58. Yoshioka M, Saiwai S, Kuroki S, Nigami H. MR imaging of the brain in Fukuyama-type congenital muscular dystrophy. *AJNR Am J Neuroradiol* 1991;12:63–66
59. Dobyns WB, Gilbert EF, Opitz JM. Further comments on the lissencephaly syndromes. *Am J Med Genet* 1985;22:197–211
60. Barkovich AJ, Truwit CL. MR of perinatal asphyxia: correlation of gestational age with pattern of damage. *AJNR Am J Neuroradiol* 1990;11:1087–1096
61. Barkovich AJ. Metabolic and destructive brain disorders. In: Barkovich AJ, ed. *Pediatric neuroimaging*. New York: Raven, 1990:35–75
62. Barkovich AJ. MR and CT evaluation of profound neonatal and infantile asphyxia. *AJNR Am J Neuroradiol* 1992;13:959–972
63. Keeney S, Adcock E, McArdle C. Prospective observations of 100 high-risk neonates by high field (1.5 tesla) magnetic resonance imaging of the central nervous system: I. Intraventricular and extracerebral lesions. *Pediatrics* 1991;87:421–430
64. Keeney S, Adcock E, McArdle C. Prospective observations of 100 high-risk neonates by high field (1.5 tesla) magnetic resonance imaging of the central nervous system: II. Lesions associated with hypoxic-ischemic encephalopathy. *Pediatrics* 1991;87:431–438
65. Baker L, Barkovich AJ. The large temporal horn: MR analysis in developmental brain anomalies versus hydrocephalus. *AJNR Am J Neuroradiol* 1992;13:115–122